Influence of the spark heat on the electrode behavior in Powder Mixed-EDM environment

M. A. Abbas[1,2,3]*, M. A. Lajis[1,2]**, A. D. Jawad[3], E. A. Rahim[1], S. Ahmad[1], N. A. J. Hosni[1]

[1] Faculty of Mechanical and Manufacturing Engineering, University Tun Hussein Onn Malaysia, 86400 Parit Raja, Johor Bahru, Malaysia
*Email: hd160087@siswa.uthm.edu.my, mohd.a.abbas1981@gmail.com
**Email: amri@uthm.edu.my, amri1970@gmail.com
Phone: +60-11-63772493
[2] Sustainable Manufacturing and Recycling Technology, Advanced Manufacturing and Materials Center (SMART-AMMC), University Tun Hussein Onn Malaysia, 86400 Parit Raja, Johor Bahru, Malaysia
[3] Engineering Technical College (ETCN), Al-Furat Al-Awsat Technical University (ATU), 54003 Main Hilla-Baghdad Road, Iraq

ABSTRACT

Most past studies did not attempt to improve the numerical model for the electrode removal rate which depends on the experimental results. Furthermore, these studies have not included the damage-sensing for the electrode in Powder Mixed-EDM (PMEDM) medium. Therefore, the current study aims to enhance this model for the copper electrode based on the heat flux for the spark channel. Besides, it focuses on sensing the copper electrode damage depending on the slope relation between eroding velocity and the pulse duration. In both studies, during machining D2 steel, Nano chromium powder in the dielectric liquid is applied. The correlation factor between the Numerical Heat Flux $q(r)$ and the experimental results for the Tool Wear Rate (TWR) attained is 93.06%. The value of this factor improves the mathematical model for TWR instead of the traditional mechanism that adopts the crater volume. Also, the damage-sensing constant (ST_D) in the copper electrode is very efficient at the minimum value of the peak current (I_P), powder concentration (P_C) and the maximum level of the pulse duration (T_{on}). Thus, the statistical confirmation using Response Surface Methodology (RSM) produced a higher value of the composite desirability (96.76%) and error percent equals to (10.3%-1.55%) and (0.18%-2.40%) for TWR and $q(r)$, respectively. On the other hand, the optimum operation values are $I_P = 10$ Amps, $T_{on} = 30$ μs, and $P_C = 2$ g/L. These confirmation values are similar to the trials No. (3) and No. (11). Therefore, these values confirm the main purpose in order to obtain the best performance for TWR at the minimum spark heat.

Keywords: D2 steel; Powder Mixed-EDM; electrode damage; heat flux of the spark channel.

INTRODUCTION

One of the best methods for cutting of metals without physical forces is the electrical discharge, where it conducts the removal operation efficiently for complex materials. This field first emerged in year 1770 and developed in 1943 to introduce the first Electrical Discharge Machining (EDM) [1]. This machine did a leap in the precise manufacturing areas especially related to airplane and aerospace [2,3]. From then, the researchers strive to improve the machining conditions of this machine. The control of the parameters of EDM represented a notable restriction to reach the advanced performance of it. Furthermore, the impedance of the dielectric liquid in the EDM machine is an obstacle to transfer the electrothermal power to the workpiece. Therefore, the material removal required high power to attain (8000 ºC – 12000ºC) and to conquer this impedance [4].

For enhancing EDM performance, the additive of powder particles to the dielectric liquid has contributed in reducing the electrical consuming [5-7]. This innovative solution led to the emergence of a new field known as Powder Mixed-EDM (PMEDM) [8,9]. This research field is treated with various responses including the wear rate of the electrode and it is considered as one of the most significant responses in PMEDM. Most of the studies proved to decrease the Tool Wear Rate (TWR) upon the addition of the powder particles to the dielectric liquid in EDM [10-12]. The mixing of the powder particles with the dielectric fluid does not represent a final solution to the problems of EDM. It is observed that both the peak current and the pulse duration with the powder concentration play an influential role in TWR. The growth of these parameters through the use of aluminum powder mixed with kerosene causes a decrease in the wear rate of the copper electrode [10]. The TWR of the copper electrode in this study has been reduced depending on the primary or significant role of the peak current and the pulse interval, but the pulse duration and powder concentration of chromium have a slight effect on TWR. This case led to obtaining the best TWR of the copper electrode [13]. The minimum concentration of B_4C and constant values of the peak current and the pulse duration produces a slight effect of eroding in the copper electrode [14]. Based on these studies on the copper electrode, the variation of the wear effect was observed. This situation attributes to the thermal conductivity of the powder used and heat transmitted to this electrode. One of the early studies has placed some interest in measuring the energy transferred in EDM environment performed on the Copper-Tungsten electrode. It was proved that this electrode absorbs (≈15% - ≈42%) of the total transferred energy from the plasma channel [15]. The conventional mechanism of heat supply in PMEDM depends on both the voltage and current supplied which does not represents the actual character of the heat transmitted [16]. Therefore, the heat flux based on Gaussian Distribution is considered the best mathematical model to understand the behavior of TWR [17,18].

The heat distribution model in EDM, according to Izquierdo's model, was adopted by the previous researchers to simulate the removing rate of both the workpiece and the electrode tool [19]. In the last decade, this model was improved to meet with PMEDM requirements [20]. The early results of this enhanced the model which became very correlated and reached 91% and 92.2% with the experimental values of the removal rate of D2 steel and BeCu alloy, respectively [20,21].

From the past studies, the significant comments related to the removal rate of electrode tool are discussed as follows:

1. The primary parameters in PMEDM field are peak current, pulse duration, and powder concentration.
2. Prolonging the pulse interval in PMEDM is an impact factor on TWR.
3. TWR is also affected by the powder properties and heat transmitted in PMEDM.
4. The novel research vision in EDM and PMEDM depends on the Gaussian distribution for the energy transferred to the workpiece and the electrode tool.

On the other hand, previous studies have highlighted the MRR response without mentioning the limitations of this response. Wherein, the increasing of MRR and precision of the removal operation are considered as significant effects for the prior researchers. However, these effects are also considered as limitations and as side effects in the electrical discharge environment. Generally, the increasing of MRR results from exposing the workpiece to an enormous mass of the spark energy. Simultaneously, this enormous energy also contributes to growing the TWR for the electrode tool [22-24]. Hence, this growth in TWR conducts to increasing the electrode tool damage and the loss of its dimensions. Therefore, the electrode has become incapable of implementing the removal operation with high precision [25]. According to these limitations, the material removal rate for the workpiece has not become the main objective for the researchers in this environment since the quality of machinability is not desirable. Thus, it is important to highlight both the wear rate of the electrode tool and the damage of it. As such, the scope of this study is established depending on the influence of spark heat on both TWR performance and the damage of the electrode tool in the PMEDM medium to enhance the performance of the electrode tool. Consequently, the present study focuses on the influence of the heat transferred to the copper electrode through machining D2 steel in PMEDM medium using the Nano Chromium Powder (NCP). The methodology of this paper depends on predicting the relation between heat flux according to Gaussian distribution and TWR. Besides, it also deals with the eroding velocity for this electrode that occurs during machining. This velocity in PMEDM relies on the radius of the plasma channel and pulse duration and employs to foretell the damage of the tool. The Multiple-Response Optimization will present a vital role to prove this case by confirming the active parameters.

METHODOLOGY

EDM-Die Sinking machine (Model AQ55L) does not contain a circulation system to mix the powder particles with the dielectric liquid as illustrated in Figure 1 (1.1). Consequently, this conventional machine is not efficient enough to be implemented in the experimental side of this study. The Integrated high Performance-EDM (IHP-EDM) system comprises of the circulation system as shown in Figure 1 (1.2) and EDM machine in Figure 1 (1.1). This system is considered as the perfect option to provide the PMEDM environment. The circulation system in IHP-EDM consists of the circulation lines that contain a magnetic filter to attract the debris and particle filter to recirculate the powder particles. These particles are then carried to the insulating tank after passing by the reservoir tank. In Figure 1 (1.3), the insulating tank is designated to ensure the mixing operation of the powder particles with

kerosene separates away from the original container of the EDM machine. Through magnification as shown in Figure 1 (1.3a), the insulating tank includes the work materials used to perform the experimental side. On the other hand, Figure 1 (1.3(b-d)) refers to the copper electrode, AISI D2 steel, and NCP particles mixed with kerosene, respectively.
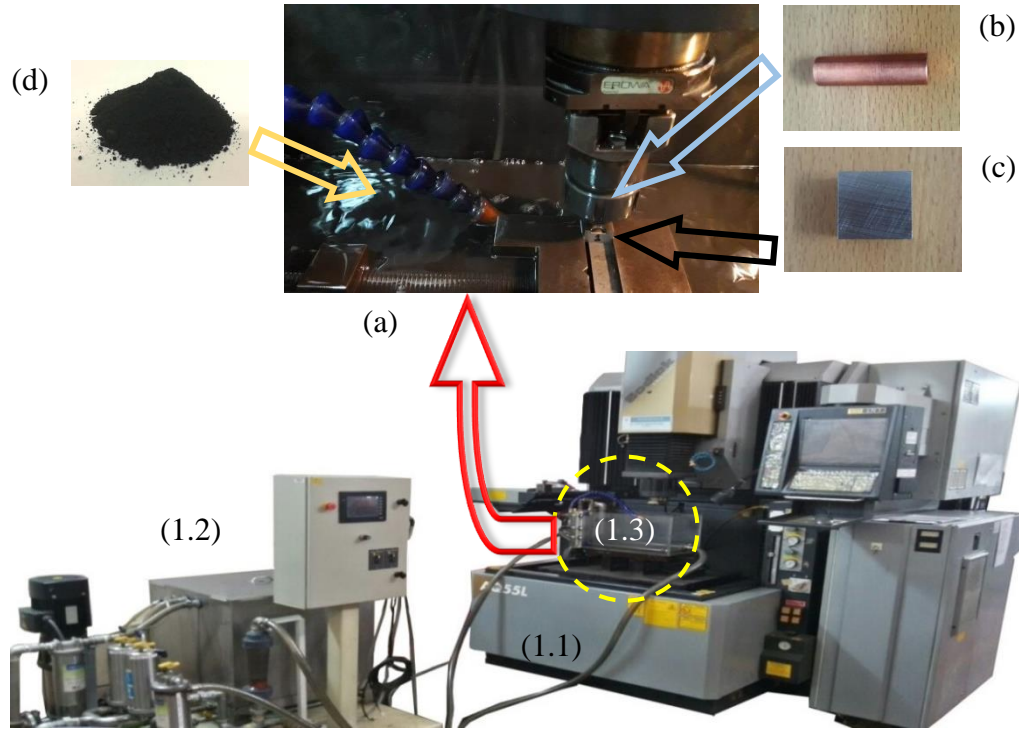

Figure 1. PMEDM environment in IHP-EDM system.
Notes: (1.1) Conventional EDM; (1.2) Circulation system; (1.3) The insulating tank that composed of: (1.3a) Magnification the insulating tank; (1.3b) Copper electrode tool; (1.3c) AISI D2 steel; (1.3d) NCP particles blended with kerosene.

Table 1 clarifies the chemical composition of D2 steel, copper electrode tool, and Nano Chromium Powder (NCP) particles used in this study, while in Table 2, properties of these work materials are illustrated. Furthermore, the significant properties of kerosene are mentioned in Table 2, besides the properties of other work material.

Table 1. Chemical composition of the workpiece, the electrode tool, and the powder particles.

Work Material	Chemical Composition
Workpiece (AISI D2)	12.8%Cr, 0.4%Si, 0.35%Mn, 0.03%P, 0.09%Ni, 0.09%Cu, 1.5%C, 0.7%Mo, 0.4% V, 0.01%Co, Fe-Balance
Electrode Tool (Cu)	0.06%Zn, 0.01%Pb, 0.01%Si, 0.02%Mn, 0.05%P, 0.02%S, 0.05%Sn, 0.07%Al, 0.03%Ni, 0.05%Sb, 0.07%Fe, Cu-Balance
Powder(Cr)	0.08%Si, 0.09%P, 0.01%S, 0.07%Cu, 0.01%C, Cr-Balance

Table 2 illustrates the properties of the work materials and the dielectric liquid, and gives a simple idea to understand the central role of NCP particles in PMEDM medium. Following from there, the electrical resistivity of NCP particles and kerosene explains this idea. Thus, the heat of the plasma channel presents enough explanation for this idea with the removal rate of the copper electrode. Furthermore, the operation concept of IHP-EDM system leads to the needing of setting the experimental conditions used to conduct this integrated system. On the other hand, Table 3 displays the experimental conditions applied in this study.

Table 2. Properties of work materials used in IHP-EDM system.

Property	Unit	Copper Electrode Tool	AISI D2 Steel Workpiece	Nano Chromium Powder	Kerosene Dielectric Fluid
Density	g/cm^3	8.99	7.7	7.16	0.728
Melting point	ºC	1084	1711	1875	
Specific heat	J/Kg/ºC	385.15	412.21	0.460	
Thermal conductivity	W/m.ºC	4.01	29	0.67	
Electrical resistivity	µΩ-cm	1.673		0.026	1.6×10^{-14}

Table 3. Experimental conditions.

Working Parameters	Descriptions
Electrode tool	Copper (Ø 10 mm)
Workpiece	AISI D2 (7.5 mm × 7.5 mm × 10 mm)
Dielectric liquid	Kerosene + Nano Chromium Powder (NCP)
Particle size of NCP	70 nm–80 nm
NCP concentration	2 g/L-6 g/L
Peak current	10 Amps- 20 Amps
Pulse duration	20 μs- 30 μs
Pulse interval	85 μs
Polarity	Negative
Voltage	120 Volt
Depth of cut	3 mm
Flushing rate	1500 mm^3/h
Machining time	30 min

Depending on the available literature in this paper, the interacted relationship between the heat flux of plasma channel q(r) and the Tool Wear Rate (TWR) in PMEDM medium is observed. Through the experimental conditions presented in Table 3, the affecting factors are the peak current (I_P), pulse duration (T_{on}), and concentration (P_C) of NCP particles. Hence, the Full Factorial technique is implemented in this study to design the experimental runs. This technique will arrange the experiments based on the following procedure:

$$N_r = (L^f \times n) + N_c \tag{1}$$

where N_r denotes the number of experimental runs, L is the number of parameters level, f is the number of parameters, n is the number of replicates for corner points, and N_c indicates the number of center points per block. Thus, the total number of runs to perform the experimental side is 19. Furthermore, Table 4 below refers to the number of trials to conduct this study. The effects of this study represent the variables that will be produced from the trials mentioned in Table 4. Through these effects, the behavior of heat on the electrode tool can be translated to enhance and develop significant relations. The first effect refers to the Tool Wear Rate (TWR) of the copper electrode given in Equation. (2) those results from the designated trials in Table 4.

$$TWR = (m_b - m_a)/\rho_e \, t_m \tag{2}$$

Here, m_b is the electrode mass before machining in PMEDM, m_a is the electrode mass after machining in PMEDM, t_m is the machining time in PMEDM, and ρ_e denotes the electrode density.

Table 4. Experimental design with the experimental and numerical outcomes for TWR and q(r), respectively.

No. of Runs	I_P (Amps)	T_{on} (µs)	P_C (g/L)	TWR (mm³/min)	q(r) (µW/µm²)
1	10	20	2	0.0902	0.0772
2	20	20	2	0.1011	0.0850
3	10	30	2	0.0634	0.0540
4	20	30	2	0.1486	0.0595
5	10	20	6	0.1072	0.2315
6	20	20	6	0.1790	0.2551
7	10	30	6	0.0826	0.1620
8	20	30	6	0.1612	0.1785
9	10	20	2	0.0902	0.0778
10	20	20	2	0.1096	0.0864
11	10	30	2	0.0718	0.0554
12	20	30	2	0.1399	0.0615
13	10	20	6	0.1007	0.2411
14	20	20	6	0.1690	0.2678
15	10	30	6	0.0776	0.1715
16	20	30	6	0.1522	0.1904
17	15	25	4	0.1072	0.1443
18	15	25	4	0.1072	0.1454
19	15	25	4	0.1194	0.1465

The other effect that we deal with in this study is the numerical model of heat flux for the spark channel. The usage of this model is not proper to investigate in PMEDM environment [19]. Therefore, this model is modified to include the powder quantity added to the dielectric liquid [20]. Besides, previous researchers agree on the same hypotheses for this model in PMEDM [20-21]. Consequently, Equations. (3)-(4) revealed the spark channel radius and the heat flux of this channel in PMEDM according to the modified model [19,20,26] given by:

$$r_s = (2.04\,e - 3)\,I_P^{\,0.43}\,T_{on}^{\,0.44} \tag{3}$$

$$q(r) = 4.57\,P_C\,H_F\,V\,I_P\,e^{-4.5(R/r_s)^2} \Big/ \pi\,r_s^{\,2} \tag{4}$$

where H_F is the heat fraction constant and equals (5%-9%) [20], V is the voltage, P_C is the powder concentration in the dielectric liquid [21], R is the polar radius, and r_s indicates the spark radius of plasma channel in PMEDM. Figure 2 above illustrates the mechanism of this channel according to the Gaussian distribution. In Figure 2, both AB and BC with CD refers to the isolated sides of the copper electrodes, while AB is considered the axisymmetric line. AE and AD clarifies the spark radius (r_s) and polar radius (R), respectively. Thus, it is observed that the boundary conditions of the spark heat in PMEDM are given by [20]:

$$k_e(\partial T/\partial z)=\begin{cases} h_m\delta T & (R \succ r_s) \\ q(r) & (R \prec r_s) \end{cases} \tag{5}$$

where h_m refers to the heat convection coefficient of the mixed dielectric fluid, δT is the change of heat temperature between this liquid and the copper electrode, and k_e is the thermal conductivity of the copper electrode.
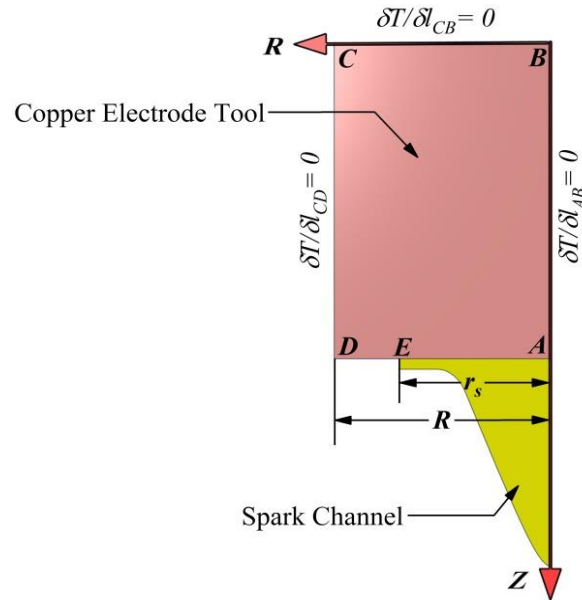
Figure 2. The symmetric heat flux according to Gaussian distribution of the plasma channel on the copper electrode in PMEDM medium.

In Equation. (5), the boundary condition at DE is based on the transient mode of the heat convection by the mixed dielectric liquid. This condition is confirmed when ($R > r_s$), whereas the other boundary condition in Equation. (5) represents the transient heat conduction of the single spark which is applied when ($R < r_s$) at AE only [20].

This brief explanation of the methodology performed in this paper has established based on the machine setup, work materials, the design of experiments, and the effects. Therefore, it is focused on to employ the results of eroding in the copper electrode using Equation. (2) with the numerical model of the heat flux according to Equation. (4). The purpose of these results is to improve the numerical model of the wear rate and to identify a new model for sensing the damage of the electrode.

RESULTS AND DISCUSSION

The execution of the experiments mentioned in Table 4 leads to providing the experimental and numerical outcomes for TWR and q(r), sequentially. Besides, Table 4 shows the results of these effects in PMEDM. Depending on these outcomes, this study will present the interpretation of the relationship between TWR and q(r). In addition, the relationship of both

peak current (I_P) and pulse duration (T_{on}) with eroding velocity of the copper electrode is presented.

Influence of Spark Heat on TWR Performance

Through viewing the results of runs (1, 3) as revealed in Table 4, the values of TWR and q(r) drops with the increase in the pulse duration ($T_{on} = 20$ µs-30 µs), whereas I_P and P_C values are constant and equals to 10 Amps and 2 g/L, respectively, in these runs as shown in Figure 3 This case attributes to the insufficient of the pulse duration for transferring the spark energy to the copper electrode [27]. Therefore, Eq. (6) interprets the spark energy in PMEDM medium [15] given by:

$$Q_S = Q_W + Q_E + Q_P + Q_d \qquad (6)$$

where Q_W is the energy received by D2 steel, Q_E is the energy transferred to the copper electrode, Q_P is the energy absorbing by nanoparticles of chromium powder, Q_d refers to the dissipated energy to overcome the electrical resistivity of kerosene.
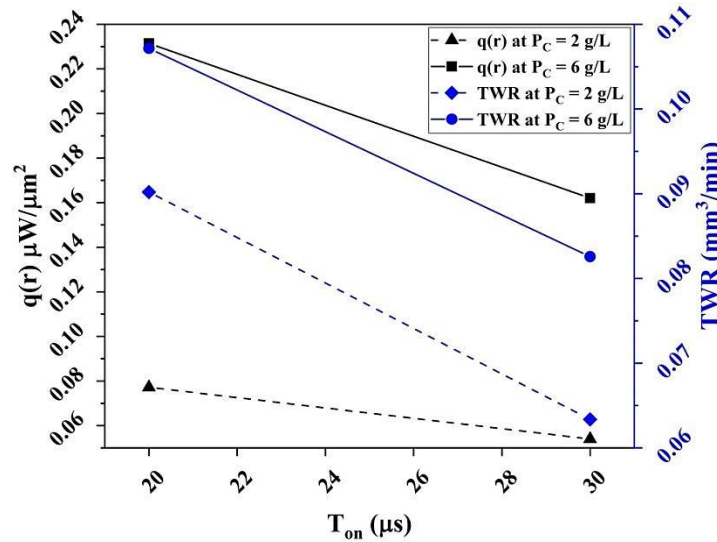

Figure 3. The influence of pulse duration (T_{on}) on the Tool Wear Rate (TWR) for the copper electrode and the numerical heat flux q(r) for the spark channel when: $I_P = 10$ Amps and $P_C = 2$ g/L; $I_P = 10$ Amps and $P_C = 6$ g/L.

The dissipated energy (Q_d) from the spark is needed to overcome the impedance of kerosene, but this energy reduces when NCP particles are added to this dielectric liquid [28]. This action led to decomposing of the kerosene and formation of compounds which then agglomerates on the surface of the copper electrode. Therefore, these compounds form a film to protect and reduce the electrical eroding of this electrode [29-31]. Besides the energy absorbing by D2 steel (Q_W), NCP particles contributes to absorbing the spark energy (Q_P) depending on the properties of these particles [14,30]. Hence, the remaining energy absorbed by the copper electrode (Q_E) is not enough to increase the TWR.

Increasing the chromium concentration to 6 g/L under the trials (5, 7) as shown in Table 4 and Figure 4 leads to increasing TWR initially at $T_{on} = 20$ µs. However, growing the pulse duration to 30 µs reduces the TWR of the copper electrode. This decreasing behavior

of TWR in the runs (5, 7) is similar to the runs (1, 3). Therefore, the interpretations of this decreasing are the same. Furthermore, this behavior is also recognized in trials (9, 11) and (13, 15), respectively.
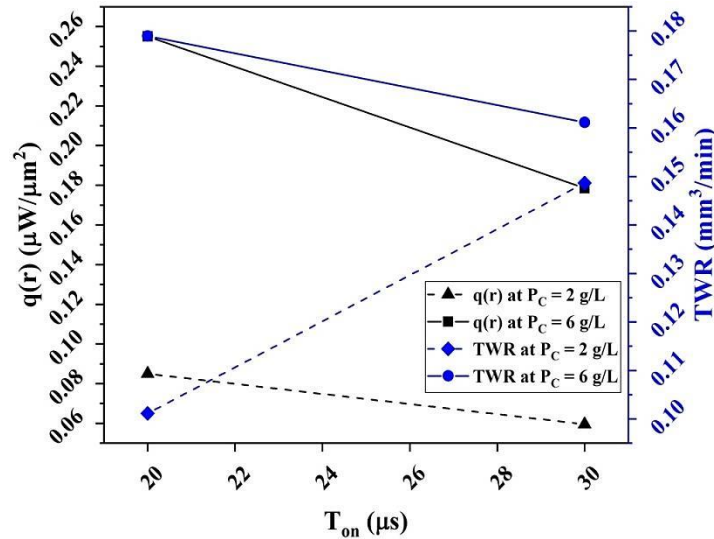

Figure 4. The influence of pulse duration (T_{on}) on the Tool Wear Rate (TWR) for the copper electrode and the numerical heat flux q(r) for the spark channel when: I_P = 20 Amps and P_C = 2 g/L; I_P = 20 Amps and P_C = 6 g/L.

The active role of NCP particles in experiments (6, 8) is continuous and reflects on the TWR for the copper electrode. Although increasing the peak current to 20 Amps, the concentration of chromium at 6 g/L is efficient to absorb the spark energy besides the absorbed energy (Q_W) by D2 steel and dissipated energy (Q_d) from breaking down the impedance of kerosene according to Eq. (6) [30]. Therefore, TWR decreases during machining when the pulse duration ranges from 20 µs to 30 µs. Figure 4 illustrates this behavior of both TWR and q(r). Additionally, the experiments 14 and 16 possess the same behavior. In contrast, P_C = 2 g/L leads to growing up of TWR with lowering of q(r). In Figure 4, this observation is seen at T_{on} = 20 µs-30 µs. The increasing of peak current to 20 Amps in trials (2, 4) due to the energy is unable to be absorbed by NCP particles, but the copper electrode is capable in absorbing this surplus [30].

Obviously, the comparisons presented in Figures 3 and 4 had not mentioned the influence of outcomes of experiments 17, 18, and 19 as compared to the comparisons implemented upon the other runs. Wherein, it is observed that these comparisons explain the influence of NCP concentrations on TWR and q(r) at 20 µs and 30 µs for every 10 Amps and 20 Amps, separately. Hence, it is remarked in Figures 3 and 4 a variance of performance for both TWR and q(r) in the PMEDM environment. Unfortunately, this variance in the experiments 17, 18, and 19 are not distinguished since the peak current, pulse duration, and concentration of NCP are fixed at 15 Amps, 25 µs, and 4 g/L, respectively. Therefore, the influence of the heat flux of the spark channel on the copper electrode in the PMEDM environment is almost convergent and moderate at these experiments, where it is impossible

to present a comparison amongst these experiments according to these fixed parameters. Thus, Table 5 presents the summary of TWR and q(r) behaviors depending on the case of parameters at each run.

Table 5. Summarizes the behavior of TWR for the copper electrode and q(r)
for spark channel depending on the run case.

Runs	T_{on} (µs)	I_P (Amps)	P_C (g/L)	Response Behavior	
				q(r)	TWR
(1,3) (5,7) (9,11) (13,15)	20,30	10	2,6	Decreased	Decreased
(6,8) (14,16)	20,30	20	6	Decreased	Decreased
(2,4) (10,12)	20,30	20	2	Decreased	Increased
(17,18,19)	25	15	4	Fair	Fair

The influence of the spark heat on the removal rate of the copper electrode is variable depending on the case of the run. It is remarked that the correlated influencing for I_P, T_{on}, and P_C parameters is due to the quantity of NCP particles must be suitable to absorb a larger magnitude of the spark energy produced from the increasing of I_P and T_{on}. Therefore, NCP particles are necessary to reduce the TWR during machining D2 steel in EDM. Figure 5 shows this correlated influencing for the responses TWR and q(r) in which the relationship produced from these responses as in Figure 5 contributes in enhancing the numerical model for the removal rate of the electrode. On the other hand, Figure 6 refers to the conventional mathematical mechanism to specify the TWR with the new procedure depending on Figure 5.
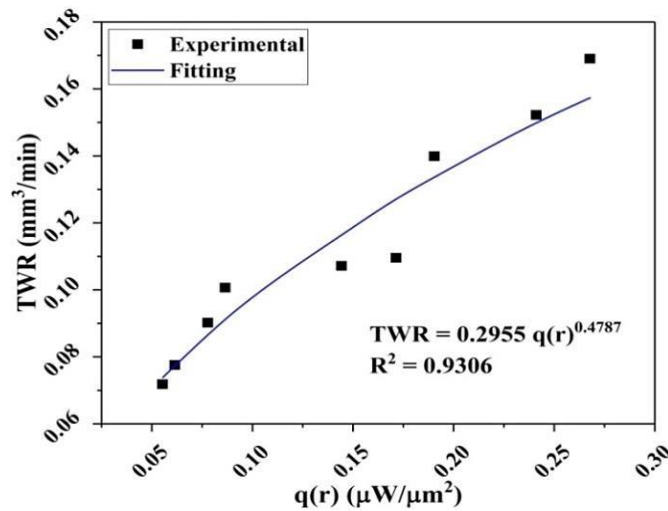

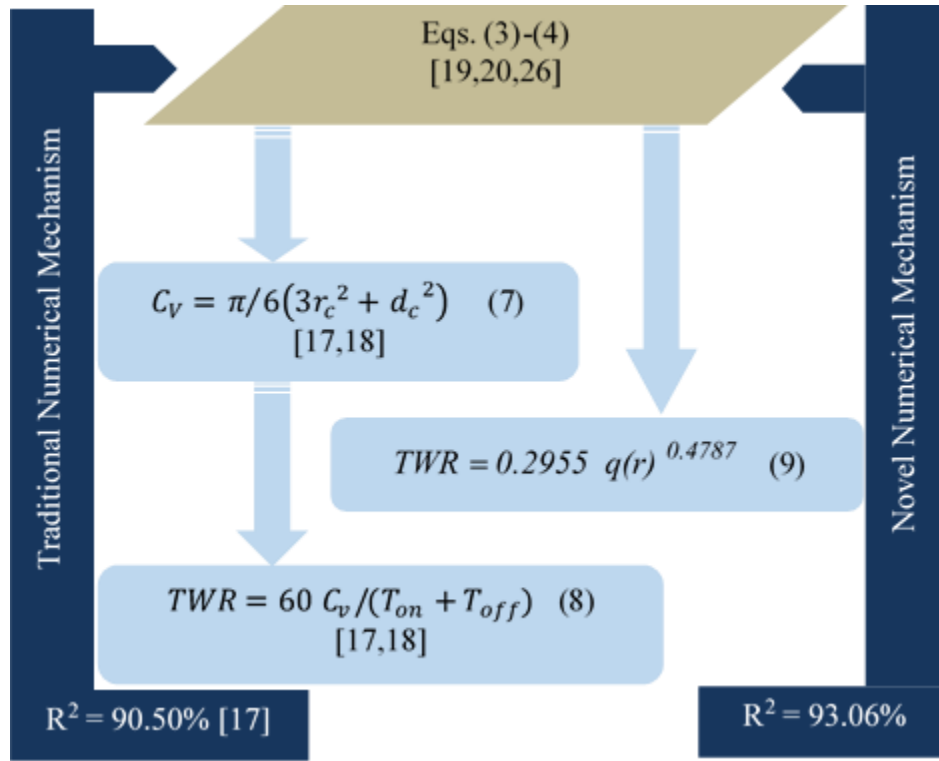Figure 5. Fitting the experimental results of both responses TWR and q(r).

Figure 6. Comparison between traditional and novel mechanisms
to specify TWR in PMEDM.

where C_V is the volume of the crater, r_C is the crater radius, d_C is the crater depth, and R^2 refers to the square of correlation factor. These symbols illustrated in Figure 6 are used along with the traditional mechanism to determine TWR for the electrode tool. R^2 was confirmed at 90.05% with the conventional procedure as shown in Figure 6 [17], but it was enhanced to be 93.06% according to the experimental results of this study. Therefore, we may utilize Equation. (9) as a validation mechanism without adopting Equations. (7)-(8) to investigate the TWR depending on the correlated influencing for this response with the heat flux of the spark channel.

Influence of the Spark Channel on the Tool Damage
In Tables 4 and 5, the spark heat has a vital role in controlling the removal rate of the copper electrode in PMEDM depending on the parameters I_P, T_{on}, and P_C. Besides, previous studies have not presented a description for sensing the damage in the electrode. The expansion or contraction of the spark channel is considered a significant behavior to increase or decrease the tool life in PMEDM environment. This behavior can be translated through Equation. (3) for determining the radius of the spark channel.

The radius of the spark channel changes with the pulse duration at the fixed peak current and this change lead to:

$$\partial r_s / \partial T_{on} = 0.8976 \, e \, I_P{}^{0.43} \, T_{on}{}^{-0.56} - 1.32 \, I_P{}^{0.43} \, T_{on}{}^{-0.56} \quad (10)$$

Based on Equation. (10), the eroding velocity (V_e) will be:

$$V_e = (0.8976 \, e \, \text{-} \, 1.32)\left(I_P{}^{0.43} / T_{on}{}^{0.56}\right) \quad (11)$$

For exploring the damage in the copper tool, the slope relation between ΔV_e and ΔT_{on} describes the damage-sensing constant for the electrode. Therefore, Equation. (12) indicates this relation in the electrical discharge environment given by:

$$m = S_{TD} = |\Delta V_e| / \Delta T_{on} \quad (12)$$

where S_{TD} denotes the damage-sensing constant for the electrode and ΔT_{on} is the change in the pulse duration used for machining in electrical discharge environment. Table 6 summarizes the values of this constant based on the change in pulse duration and peak current adopted in this study.

Table 6. Summarizes the values of the damage-sensing constant for the electrode depending on pulse duration.

Case No.	Runs	I_P (Amps)	ΔT_{on} (µs)	ΔV_e (µm/µs)	S_{TD} (µm/µs^2)
1	(1,3) (5,7) (9,11) (13,15)	10	10	0.11436	0.011436
2	(2,4) (6,8) (10,12) (14,16)	20	10	0.15407	0.015407

In Figure 7, the eroding velocity of the copper electrode at $T_{on} = 30$ µs is less than the velocity at $T_{on} = 20$ µs. Accordingly, this velocity plays a significant role to determine the damage in the tool by S_{TD} constant, whereas the radius of the spark channel in the electrical discharge medium is the base for this velocity. Thus, this velocity is very active at $I_P = 20$ Amps as illustrated in Figure 7. Following from there, the best sensitivity is achieved with S_{TD} at case (1) as shown in Table 6. The variation between cases (1) and (2) for the trials performed in this study attributes to I_P and T_{on} values depending on Equations. (11)-(12). Hence, case (1) has the priority to sense the damage in the copper electrode due to the high level of peak current being not adopted. Furthermore, a maximum value of the pulse duration is not sufficient to cause the noted damage in the copper electrode [10,32].

Both influences of heat and radius of spark channel in PMEDM based on the results of this study led to the new relations represented by Equations. (9)-(12). These relations led to improved TWR for the copper electrode and eroding mechanism for this electrode. But, the confirmation of these results will boost these influence's outcomes. Therefore, Minitab 18 is capable in supplying a statistical environment to perform the Multiple-Objective Optimization for TWR and q(r). The *Composite Desirability* (*D*) value in this paper builds from the minimum values of these responses. Consequently, the function of *D* value is given by [33-35]:

$$D = (d_1 d_2 ..... d_m)^{1/m} = \left[\prod_{i=1}^{m} d_n\right]^{1/m} \quad (13)$$

$$d_n = \begin{cases} 1 & (R_n \prec T_n) \\ \left(\dfrac{M_n - R_n}{M_n - T_n} \right)^w & (T_n \le R_n \le M_n) \\ 0 & (R_n \succ M_n) \end{cases} \tag{14}$$

where d_n is the sub-desirability, M_n is the maximum boundary for the desired response, R_n is the desired response, T_n is the target for the desired response, w is the weight factor ($w = 1$), and m refers to the number of responses.
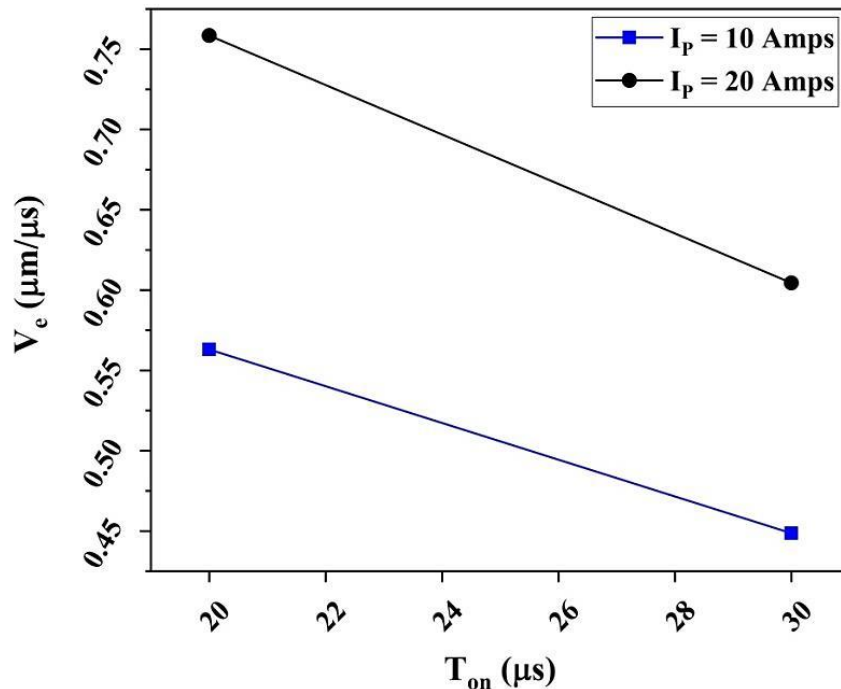

Figure 7. Variation between cases (1) and (2) for damage sensing in the copper electrode at: $I_P = 10$ Amps; $I_P = 20$ Amps.

In Figure 8, *D* value for TWR and q(r) depending on the Response Surface Methodology (RSM) is 96.76%. This value is achieved by Multiple-Response Optimization technique for these responses. The error percentage between experimental and optimal values for TWR is 10.3% and 1.55%, respectively, whereas, this percentage for q(r) is 0.18% and 2.4% amongst the numerical and predicted values, respectively. These values are shown in Table 7 and are more validated for these responses with the trials (3) and (11) in Table 4, sequentially. Thus, this confirmation achieves the best-predicted outcomes at the lowest values for TWR and q(r). Additionally, this confirmation showed minimal influence on both the heat and the radius of the spark channel on the copper electrode as above-mentioned in Tables 5 and 6. Following from there, the optimal and experimental parameters are $I_P = 10$ Amps, $T_{on} = 30$ μs, and $P_C = 2$ g/L as observed in Table 7 and Figure 8. Then, S_{TD} senses the minimum and maximum values of the peak current and the pulse duration, respectively, in PMEDM environment and lead to obtaining a logical value of this sensing. In other words, this sensing with TWR and q(r) are significant at lower level of these variables.
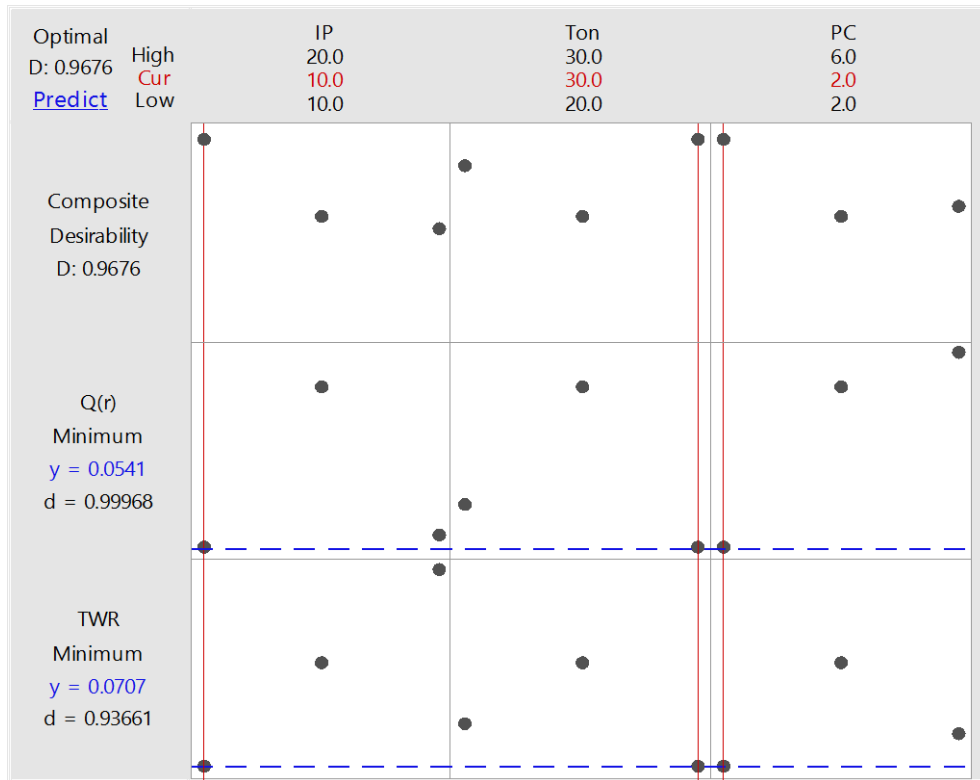
Figure 8. Optimization results and desirability for TWR and q(r).

Table 7. Conformation test and comparison with outcomes.

Optimum Operation Conditions			Experimental Operation Conditions			TWR (mm³/min)		
I_P (Amps)	T_{on} (µs)	P_C (g./L)	I_P (Amps)	T_{on} (µs)	P_C (g/L)	Predicted Value	Experimental Value	Error (%)
10	30	2	10	30	2	0.0707	0.0634	10.3%
			Similar Trial No. 3 and No. 11				0.0718	1.55%
Optimum Operation Conditions			**Experimental Operation Conditions**			**q(r) (µW/µm²)**		
I_P (Amps)	T_{on} (µs)	P_C (g./L)	I_P (Amps)	T_{on} (µs)	P_C (g/L)	Predicted Value	Experimental Value	Error (%)
10	30	2	10	30	2	0.0541	0.0540	0.18%
			Similar Trial No. 3 and No. 11				0.0554	2.40%

CONCLUSIONS

This paper presents the study of the correlated influencing between the numerical model of heat flux based on Gaussian distribution and the removal rate of the copper electrode in EDM environment using nanoparticle of chromium powder for machining D2 steel. Furthermore, this article proposes a mathematical interpretation of the damage-sensing occurring in the copper electrode as a new behavior to predict the eroding velocity in this electrode. Consequently, this study concluded the following:

1. Increasing Nano chromium particles concentration in the dielectric liquid leads to growing up of TWR for the copper electrode initially, but rising the pulse duration leads up to reducing the level of TWR for this electrode. Besides, it is observed that the value of TWR differs based on the level of the peak current used during machining.

2. Both values of the pulse duration of 20 µs and 30 µs are not enough to transfer the energy to the copper electrode. Thus, the removal rate of this electrode decreases.

3. The amount of chromium powder added in EDM medium plays an influential role to absorb the surplus energy of the spark channel resulted from increasing the peak current. Hence, this increase in the peak current leads the need to add an adequate amount of this powder to absorb this energy. Consequently, the amount of this powder is responsible for controlling the removal rate of the copper electrode.

4. Depending on the experimental and numerical outcomes for TWR and q(r), respectively, the correlation factor for these responses is 93.06%. The value of this correlation is due to enhancement in the numerical model for TWR based on the heat flux of the spark channel instead of the traditional mechanism that relies on the crater volume.

5. The eroding velocity in the copper electrode that results from the radius of the spark channel plays a significant function for sensing of the electrode damage. Hence, the increasing peak current with growing pulse duration leads to the rising of this velocity. Thus, increases the constant of sensing-damage (S_{TD}) value in this electrode.

6. The best level of STD-value is produced from the lower value of peak current with increasing pulse duration for eroding the copper electrode. Consequently, the minimum values of TWR and q(r) responses are more valuable and efficient at a minimal level for STD-value.

7. The confirmation between the performance of the damage-sensing constant and the influence of the heat for the spark channel on the copper electrode is achieved by multiple-objective prediction. This prediction is based on the Response Surface Methodology (RSM) technique to specify a Composite Desirability (D). The value of this desirability attained is 96.76% with optimum values for responses and parameters for eroding the copper electrode. The minimum level of the responses are at TWR = 0.0707 mm^3/min and q(r) = 0.0541 µW/µm^2 with error percentage for these responses ranging between 10.3%-1.55% and 0.18%-2.40%, respectively. The optimum values for applied parameters are I_P = 10 Amps, T_{on} = 30 µs, and P_C = 2 g/L. This prediction implies that the optimum values for the responses and parameters are similar to the trials No. (3) and No. (11). Besides, these optimum values translate the minimum influences of both the spark heat and the damage-sensing constant on the copper electrode.

Based on these conclusions, this study proposes to avoid sensing the high damage in the electrode tool in PMEDM environment using the minimum value of the peak current and powder concentration with the maximum level of the pulse duration. This significant levels lead to minimizing the influence of the spark heat on the electrode and produces the best performance for the eroding.

ACKNOWLEDGMENTS

REFERENCES

[1]   Chaudhury P, Samantaray S, Sahu S. Multi response optimization of powder additive mixed electrical discharge machining by Taguchi analysis. In: 5th International Conference of Materials Processing and Characterization, Hyderabad, India. 2017:2231–2241.

[2]   Khan MAR, Rahman MM, Kadirgama K, Maleque MA, Ishak M. Prediction of surface roughness of Ti-6Al-4V in electrical discharge machining: A regression model. Journal of Mechanical Engineering and Sciences. 2011;1:16–24.

[3]   Ali MY, Banu A, Salehan M, Adesta EYT, Hazza M, Shaffiq M. Dimensional accuracy in dry micro wire electrical discharge machining. Journal of Mechanical Engineering and Sciences. 2018;12:3321–9.

[4]   Tripathy S, Tripathy DK. Multi-response optimization of machining process parameters for powder mixed electro-discharge machining of H-11 die steel using grey relational analysis and topsis. Machining Science and Technology. 2017;21:362–384.

[5]   Shard A, Shikha D, Gupta V, Garg MP. Effect of B_4C abrasive mixed into dielectric fluid on electrical discharge machining. Journal of the Brazilian Society of Mechanical Sciences and Engineering. 2018;40:1-11.

[6]   Luzia CAO, Laurindo CAH, Soares PC, Torres RD, Mendes LA, Amorim FL. Recast layer mechanical properties of tool steel after electrical discharge machining with silicon powder in the dielectric. The International Journal of Advanced Manufacturing Technology. 2019;103:15–28.

[7]   Kumar A, Mandal A, Dixit AR, Das AK, Kumar S, Ranjan R. Comparison in the performance of EDM and NPMEDM using Al_2O_3 nanopowder as an impurity in DI water dielectric. The International Journal of Advanced Manufacturing Technology. 2019;100:1327–39.

[8]   Kansal HK, Singh S, Kumar P. Technology and research developments in powder mixed electric discharge machining (PMEDM). Journal of Materials Processing Technology. 2007;184:32–41

[9]   Kansal HK, Singh S, Kumar P. Effect of silicon powder mixed EDM on machining rate of AISI D2 die steel. Journal of Manufacturing Processes. 2007;9:13–22.

[10]   Roy C, Syed KH, Kuppan P. Machinability of Al/10% SiC/25% TiB2 metal matrix composite with powder-mixed electrical discharge machining. In: 1st Global Colloquium on Recent Advancements and Effectual Researches in Engineering, Science and Technology, Palai, India. 2016;1056–1063.

[11]   Prakash et al. Experimental investigations in powder mixed electric discharge machining of Ti-35Nb-7Ta-5Zrβ-titanium alloy. Materials and Manufacturing Processes. 2017;32: 274–285.

[12]   Syed KH, Palaniyandi K. Performance of electrical discharge machining using aluminum powder suspended distilled water. Turkish J. Eng. Environ. Sci. 2012;36:195–207.

[13]   Abrol A, Sharma S. Effect of chromium powder mixed dielectric on performance characteristic of AISI D2 die steel using EDM. International Journal of Research in Engineering and Technology. 2015;4:232–246.

[14]   Kolli M, Kumar A. Effect of boron carbide powder mixed into dielectric fluid on electrical discharge machining of titanium alloy. In: International Conference on Advances in Manufacturing and Materials Engineering, Karnataka, India. 2014:1957–1965.

[15]   Singh H. Experimental study of distribution of energy during EDM process for utilization in thermal models. International Journal of Heat and Mass Transfer. 2012; 55:5053–5064.

[16]   Ali MY et al. Powder mixed micro electro discharge milling of Titanium alloy: Analysis of surface roughness. Advanced Materials Research. 2012;341-342: 142-146.

[17]   Liu Y et al. The simulation research of tool wear in small hole EDM machining on Titanium alloy. Applied Mechanics and Materials. 2014;624:249-254.

[18]   Sanghani CR, Acharya GD, Kothari KD. Finite element analysis of tool wear rate in electrical discharge machining and comparison with experimental results. Trends in Machine Design. 2016;3:18–22.

[19]   Izquierdo B et al. A numerical model of the EDM process considering the effect of multiple discharges. International Journal of Machine Tools and Manufacture. 2009;49:220–229.

[20]   Kansal HK, Singh S, Kumar P. Numerical simulation of powder mixed electric discharge machining (PMEDM) using finite element method. Mathematical and Computer Modelling. 2008;47:1217–1237.

[21]   Jatti VS, Bagane S. Thermo-electric modeling, simulation and experimental validation of powder mixed electric discharge machining (PMEDM) of BeCu alloys. Alexandria Engineering Journal. 2017;57: 643-653.

[22]   Khan A. A. Electrode wear and material removal rate during EDM of aluminum and mild steel using copper and brass electrodes. The International Journal of Advanced Manufacturing Technology. 2008; 39:482–487.

[23]   Patel S, Thesiya D, Rajurkar A. Aluminium powder mixed rotary electric discharge machining (PMEDM) on Inconel 718. Australian Journal of Mechanical Engineering. 2018;16:21–30.

[24]   Jawahar M, Reddy CS, Srinivas C. A review of performance optimization and current research in PMEDM. Materials Today: Proceedings. 2019.

[25]   Khan AA, Mridha S. Performance of Copper and Aluminum Electrodes during EDM of Stainless Steel and Carbide. Journal for Manufacturing Science and Production. 2006;7:1–8.

[26]   Joshi SN, Pande SS. Thermo-physical modeling of die-sinking EDM process. Journal of Manufacturing Processes. 2010; 12:45–56.

[27]   Long BT et al. Optimization of PMEDM process parameter for maximizing material removal rate by Taguchi's method. The International Journal of Advanced Manufacturing Technology. 2016;87:1929–1939.

[28]   Kumar S, Batra U. Surface modification of die steel materials by EDM method using tungsten powder-mixed dielectric. Journal of Manufacturing Processes. 2012;14:35–40.

[29]   Bhatt G, Batish A, Bhattacharya A. Experimental investigation of magnetic field assisted powder mixed electric discharge machining. Particulate Science and Technology. 2015;33:246–256.

[30]   Batish A, Bhattacharya A, Kumar N. Powder mixed dielectric: an approach for improved process performance in EDM. Particulate Science and Technology. 2015;33:150–158.

[31]   Shabgard MR, Kabirinia F. Effect of dielectric liquid on characteristics of WC-Co powder synthesized using EDM process. Materials and Manufacturing Processes. 2014;29:1269–1276.

[32]   Rathi MG, Mane DV. Study on effect of powder mixed dielectric in EDM of Inconel 718. International Journal of Scientific and Research. 2014;4:1–7.

[33]   Del Castillo E, Montgomery DC, McCarville DR. Modified desirability functions for multiple response optimization. Journal of Quality Technology. 1996;28:337–345.

[34]   Myers RH, Montgomery DC, Anderson-Cook CM. Response surface methodology: Process and product optimization using designed experiments. 3rd. New Jersey: John Wiley and Sons; 2016.

[35]   Ali MY, Moudood MA, Maleque MA. Electro-discharge machining of alumina: Investigation of material removal rate and surface roughness. Journal of Mechanical Engineering and Sciences. 2017;11:3015-3026.